

# Mechanism of DNA Binding Enhancement by Hepatitis B Virus Protein pX<sup>†</sup>

C. Rodgers Palmer,<sup>‡</sup> Laura D. Gagnas,<sup>§</sup> and Alanna Schepartz<sup>\*,§</sup>

Departments of Chemistry and of Molecular Biophysics and Biochemistry, Yale University,  
New Haven, Connecticut 06520-8107

Received August 21, 1997; Revised Manuscript Received October 10, 1997<sup>®</sup>

**ABSTRACT:** At least three hundred million people worldwide are infected with the hepatitis B virus (HBV), and epidemiological studies show a clear correlation between chronic HBV infection and the development of hepatocellular carcinoma. HBV encodes a protein, pX, which abducts the cellular transcriptional machinery in several ways including direct interactions with bZIP transcription factors. These interactions increase the DNA affinities of target bZIP proteins in a DNA sequence-dependent manner. Here we use a series of bZIP peptide models to explore the mechanism by which pX interacts with bZIP proteins. Our results suggest that pX increases bZIP•DNA stability by increasing the stability of the bZIP dimer as well as the affinity of the dimer for DNA. Additional experiments provide evidence for a mechanism in which pX recognizes the composite structure of the peptide•DNA complex, not simply the primary peptide sequence. These experiments provide a framework for understanding how pX alters the patterns of transcription within the nucleus. The similarities between the mechanism proposed for pX and the mechanism previously proposed for the human T-cell leukemia virus protein Tax are discussed.

Infection with the hepatitis B virus results in chronic hepatitis B, and epidemiological studies show a clear correlation between chronic HBV<sup>1</sup> infection and the development of hepatocellular carcinoma (1). The HBV genome encodes surface and core antigens (2, 3), a viral polymerase (4), and a protein called pX that is highly conserved among hepadnaviridae (5). Though not the product of an oncogene, pX induces the malignant transformation of fetal mouse cells (6) and is implicated in the progression from HBV infection to liver cancer (7). In spite of its importance in the etiology of hepatocellular carcinoma, the molecular basis for pX function remains poorly understood.

pX functions in both the cytoplasm and the nucleus (8). In the cytoplasm, pX stimulates the Ras-Raf-MAP kinase signaling cascade by increasing the fraction of active, GTP-bound Ras (9). The result is an increased fraction of active Raf and mitogen-activated protein kinase which can stimulate transcriptional activators. In the nucleus, pX stimulates transcription from a variety of DNA target sites including the SRE (10),  $\kappa$ B (11), C/EBP, HBV and HTLV enhancers (12), AP-1 and AP-2 (13), SV40 (14), and CRE (15). Although in certain cases pX may enhance transcription by stimulating phosphorylation cascades (9), in other cases there is evidence for a direct pX–transcription factor interaction (16–21). pX does not possess high intrinsic DNA affinity (17, 22), yet it activates transcription from multiple DNA

target sites. These observations suggest that pX interacts with transcription factors to enhance, directly or indirectly, their transactivation potentials (16) or to deliver the trans-activation region of pX to the DNA target (23).

Among the proteins with which pX interacts are bZIP transcription factors (24–26) in the CREB/ATF subfamily (16, 17, 27). CREB/ATF bZIP proteins mediate the cellular response to cyclic AMP by stimulating transcription from target sites containing the cAMP response element (28, 29). Early studies demonstrated that in the absence of pX, the human proteins CREB and ATF-2 bound poorly to a CRE-like site within the HBV enhancer. However, both proteins bound the HBV enhancer with high affinity in the presence of pX (17). Later biochemical studies (16) identified the bZIP element (30), the 60 amino acids that comprise the bZIP DNA binding domain (31–33), as the primary site of interaction with pX. These experiments failed to provide evidence for an increased concentration of CREB homodimer in the presence of pX, suggesting that pX did not alter the bZIP monomer–dimer equilibrium.

Based on these results, we formulated three detailed models to describe the effect of pX on the stability of a bZIP•DNA complex. These models are illustrated schematically and as free energy diagrams in Figure 1. In model 1, pX stabilizes the bZIP•DNA complex by stabilizing interactions between two bZIP monomers (34). In this model, pX stabilizes the bZIP dimer, decreasing its dissociation constant  $K_{\text{dim}}$ . In the absence of an additional effect on  $K_{\text{dna}}$ , the dissociation constant of the bZIP dimer•DNA complex, this increase in bZIP dimer stability results in an identical increase in protein•DNA complex stability ( $\Delta\Delta G_{\text{obs}}$ ). In model 2, pX stabilizes the bZIP•DNA complex by stabilizing interactions between the bZIP peptide and DNA. In this model, pX stabilizes the bZIP•DNA complex, decreasing  $K_{\text{dna}}$ . In model 3, pX stabilizes interactions between two bZIP monomers as well as interactions between the bZIP dimer and DNA to decrease both  $K_{\text{dim}}$  and  $K_{\text{dna}}$ . In this case, the observed decrease in the free energy of the bZIP•DNA

<sup>†</sup> This work was supported by the NIH (GM 53829), with additional support provided by The National Foundation for Cancer Research and Sigma Xi (GIAR 23045). C.R.P. and L.D.G. were supported by NSF Predoctoral and NIH Postdoctoral Fellowships (1-F32-GM17858-01), respectively.

\* To whom correspondence should be addressed. Phone: 203-432-5094. Fax: 203-432-6144. E-mail: alanna@milan.chem.yale.edu.

<sup>‡</sup> Department of Molecular Biophysics and Biochemistry.

<sup>§</sup> Department of Chemistry.

<sup>®</sup> Abstract published in *Advance ACS Abstracts*, November 15, 1997.

<sup>1</sup> Abbreviations: HBV, hepatitis B virus; HTLV-I, human T-cell leukemia virus type I; CRE, cyclic AMP response element; bZIP, basic region–leucine zipper; MALDI, matrix-assisted laser desorption and ionization.

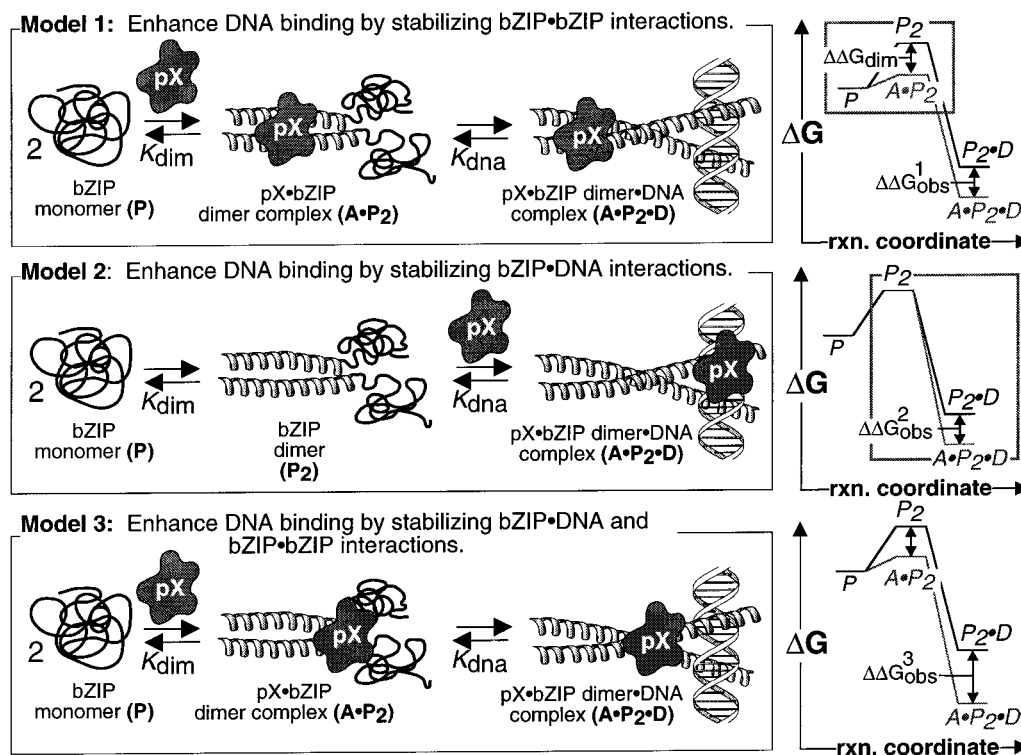


FIGURE 1: Three models to describe the effect of pX on the stabilities of bZIP•DNA complexes at equilibrium. Each model is represented by a scheme (at left) and a reaction coordinate diagram (at right). In model 1, pX increases the stability of a bZIP•DNA complex by stabilizing bZIP•bZIP interactions. In model 2, pX increases the stability of a bZIP•DNA complex by stabilizing bZIP•DNA interactions. In model 3, pX increases the stability of a bZIP•DNA complex by stabilizing bZIP•bZIP and bZIP•DNA interactions.

complex ( $\Delta\Delta G_{\text{obs}}$ ) represents the sum of the effects on dimerization and DNA binding. Here we show that the interactions between bZIP peptides and pX are most accurately depicted by model 3. Using these models and experiments with different DNA target sequences, we further identify that the structure of the basic segment bound in the major groove is an important feature recognized by pX. The ability of pX to enhance differentially the binding of proteins to varied DNA target sites provides a molecular rationale for the altered transcriptional patterns observed in HBV-infected cells (35, 36) and provides a framework for the design of pX inhibitors.

## MATERIALS AND METHODS

**HBV pX Expression and Purification.** Full-length HBV pX (subtype adw2) was expressed in BL21(DE3) pLysS *E. coli* from a pET-8c plasmid (37), and purified (16, 37). After purification, the solution containing pX was dissolved in 0.05% (v/v) aqueous NP-40 at a concentration of 48  $\mu\text{M}$ , aliquoted into single-use fractions, and stored at  $-70^\circ\text{C}$ . The fraction of active pX in our preparation was not determined. Analogous treatment of BL21(DE3) pLysS cells transformed with pBR322 did not produce any observable protein, nor activity in the electrophoretic mobility shift assays (EMSA) described below.

**Peptides and DNA.** The preparation and purification of peptides G<sub>54</sub> (38) and G<sub>29</sub><sup>SS</sup> (39, 40) have been described, as have DNA duplexes CRE<sub>24</sub> and AP<sub>123</sub> (39, 40). G<sub>56</sub> was a kind gift of Dr. Tom Ellenberger (Harvard University, School of Medicine). The DNA duplexes CRE<sub>33</sub>, HBV<sub>33</sub>, CHC<sub>33</sub>, and HCH<sub>33</sub> contained the following sequences: CRE<sub>33</sub>: 5'-CTCTGCGTGGAGATGACGTCATCTCGTCTCTGC-3', HBV<sub>33</sub>: 5'-CTCTGCTGTTTGCTGACGCAAC-

CCCCACTCTGC-3', CHC<sub>33</sub>: 5'-CTCTGCGTGGAGCTGACGCAACCTCGTCTCTGC-3', HCH<sub>33</sub>: 5'-CTCTGCTGTTTGATGACGTCATCCCCACTCTGC-3', and their complements. Synthetic oligonucleotides were purified and 5'-end-labeled by use of standard methods (41).

The peptide A<sub>65</sub> contains ATF-2 residues 347–411 fused to a carboxy-terminal hexa-histidine tag to aid in purification (27). A<sub>65</sub> was expressed in BL21(DE3) pLysS *E. coli* from plasmid pLGA65. The cell pellet was suspended in 10 mL of 50 mM NaH<sub>2</sub>PO<sub>4</sub>, 300 mM NaCl, and 10 mM 2-mercaptoethanol (pH 8.0), lysed by boiling, and clarified by centrifugation. A<sub>65</sub> was purified by Ni chelate chromatography (Qiagen) and dialyzed against 10 mM KH<sub>2</sub>PO<sub>4</sub>, 2.5 mM 2-mercaptoethanol (pH 7.4) before use. MALDI mass spectrometry indicated a molecular mass of 8701 Da for the isolated peptide, which agreed well with the expected mass of A<sub>65</sub>, 8605 Da.

Peptide A<sub>32</sub> was prepared by solid-phase synthesis using standard Fmoc/TBTU amino acid chemistry and a Millipore 9600 Peptide Synthesizer (42). Cleavage of the peptide from the solid support required 4 h at 25  $^\circ\text{C}$  in 5 mL of a solution containing 84% TFA, 4% phenol, 4% water, 4% ethanedithiol, and 4% thioanisole. The peptide was purified by reverse-phase HPLC on a semi-preparative C<sub>18</sub> 300 Å column (Vydac). MALDI mass spectrometry indicated a molecular mass of 4314 Da for the isolated peptide, which agreed well with the expected mass of A<sub>32</sub>, 4292 Da. A<sub>32</sub><sup>SS</sup> was prepared by air oxidation of A<sub>32</sub>, and purified by HPLC as described for A<sub>32</sub>.

**Electrophoretic Mobility Shift Assay.** These experiments were performed as described (43). A set of solutions containing serially diluted bZIP peptide was incubated with <50 pM DNA in the presence or absence of 9.7  $\mu\text{M}$  pX in

	Basic Region	Spacer	Leucine Zipper
A <sub>65</sub>	MNEDPDEKRRKFLERNRAAASRCRQKRKVWVQSLEKKAEDLSSLNGQLQSEVTLLRNEVAQLKQLLHHHHH		
A <sub>32</sub>	MNEDPDEKRRKFLERNRAAASRSRQKRKVWVQSGGC		
G <sub>56</sub>	MKDPAAALKRARNTAARRSRARKLQRMKQLEDKVEELLKSNYHLENEVARLKKLVGER		
G <sub>54</sub>	SAALKRARNTAARRSRARKLQRMKQLEDKVEELLKSNYHLENEVARLKKLVGER		
G <sub>29</sub>	SAALKRARNTAARRSRARKLQRMKQGGC		

FIGURE 2: bZIP peptides used in this study. The DNA binding activity of a bZIP protein is localized to 60 contiguous amino acids termed the bZIP element (30–32, 60). Each bZIP element contains three segments: a zipper segment that mediates formation of a parallel coiled coil from two protein monomers (61); a basic segment containing residues that contact DNA (62, 63); and a spacer segment that fixes the relative orientation of the basic and zipper segments (64, 65) and contributes to half-site spacing selectivity (31, 38, 66, 67).

a reaction mixture containing 2.7 mM KCl, 137 mM NaCl, 4.8 mM Na<sub>2</sub>HPO<sub>4</sub>, 1.4 mM KH<sub>2</sub>PO<sub>4</sub>, 1 mM EDTA (pH 7.8), 1 mM DTT, 0.034% (v/v) NP-40, 10% (v/v) glycerol, 1  $\mu$ g of BSA, and 40 ng of poly(dI·dC)·poly(dI·dC) in a final volume of 10  $\mu$ L. DTT was omitted in reactions containing A<sub>32</sub><sup>SS</sup> or G<sub>29</sub><sup>SS</sup>. Reactions were incubated for 45 min at either 25 °C or 4 °C, and then applied directly onto nondenaturing 10% [49:1 acrylamide:bis(acrylamide) ratio] gels prepared in 20 mM Tris, 153 mM glycine. Incubation of the binding reactions for times up to 2 h yielded results that were identical to those obtained using a 45 min incubation, indicating that the reactions reached equilibrium within 45 min. Data were quantitated as described previously (43).

## RESULTS

**Effect of pX on Dimerization and DNA Binding of bZIP Proteins.** To determine which of the three proposed models best describes the mechanism of DNA binding enhancement by HBV pX, we compared the effect of pX on the DNA affinities of two peptides, A<sub>65</sub> and A<sub>32</sub><sup>SS</sup>. Both peptides were derived from human ATF-2 (27, 44). A<sub>65</sub> contained the entire ATF-2 bZIP element, whereas A<sub>32</sub><sup>SS</sup> contained two copies of the ATF-2 basic and spacer segments (Figure 2) joined at their carboxy termini by a disulfide bond. Since A<sub>32</sub><sup>SS</sup> is a covalent dimer in the absence of pX, it is insensitive to a pX-induced increase in dimer concentration. Thus, if pX stabilizes the A<sub>65</sub>·DNA complex solely through an increase in the stability of the bZIP dimer (model 1), then A<sub>65</sub> should display higher DNA affinity in the presence of pX whereas A<sub>32</sub><sup>SS</sup> should not. If pX stabilizes the A<sub>65</sub>·DNA complex solely through an increase in the stability of A<sub>65</sub>·DNA interactions (model 2), then both A<sub>65</sub> and A<sub>32</sub><sup>SS</sup> should display higher DNA affinity in the presence of pX and the magnitudes of the enhancements should be comparable. Finally, if pX stabilizes the A<sub>65</sub>·DNA complex by increasing the stability of the bZIP dimer as well as the stability of bZIP·DNA interactions (model 3), then both A<sub>65</sub> and A<sub>32</sub><sup>SS</sup> should display higher DNA affinity in the presence of pX. However, the effect on A<sub>65</sub> should be greater than the effect on A<sub>32</sub><sup>SS</sup> by the amount corresponding to the effect on peptide dimerization (43).

**pX Stabilizes bZIP·bZIP and bZIP·DNA Interactions.** Binding isotherms illustrating the affinities of A<sub>65</sub> and A<sub>32</sub><sup>SS</sup> for a 24 bp oligonucleotide (CRE<sub>24</sub>) containing a consensus CRE site (ATGACGTCAT) in the presence and absence of 9.7  $\mu$ M pX are shown in Figure 3A. Equilibrium dissociation constants and the corresponding binding free energies are summarized in Table 1. pX supplemented the free energy of the A<sub>65</sub>·CRE<sub>24</sub> complex by  $\Delta\Delta G_{\text{obs}} = -1.7 \pm 0.2$  kcal·mol<sup>-1</sup> under conditions where it supplemented the free energy of the A<sub>32</sub><sup>SS</sup>·CRE<sub>24</sub> complex by  $\Delta\Delta G_{\text{obs}} = -0.8 \pm$

0.1 kcal·mol<sup>-1</sup>. Thus, the affinities of both A<sub>65</sub> and A<sub>32</sub><sup>SS</sup> for CRE<sub>24</sub> were enhanced by pX, but the effect on A<sub>65</sub> was approximately twice the effect on A<sub>32</sub><sup>SS</sup>. Decreasing the pX concentration to 1.2  $\mu$ M decreased the magnitudes of the observed free energy changes; however, the ratio between the  $\Delta\Delta G_{\text{obs}}$  values observed for A<sub>65</sub> and A<sub>32</sub><sup>SS</sup> was unchanged (data not shown). Similar results were obtained with an analogous set of peptides derived from the yeast protein GCN4 (45) (G<sub>54</sub> and G<sub>29</sub><sup>SS</sup>) (Figure 2): pX supplemented the free energy of the G<sub>54</sub>·CRE<sub>24</sub> complex by  $\Delta\Delta G_{\text{obs}} = -2.2 \pm 0.3$  kcal·mol<sup>-1</sup> under conditions where it supplemented the free energy of the G<sub>29</sub><sup>SS</sup>·CRE<sub>24</sub> complex by  $\Delta\Delta G_{\text{obs}} = -0.7 \pm 0.1$  kcal·mol<sup>-1</sup>. Taken together, these results indicate that the effect of pX on DNA binding by ATF-2- and GCN4-derived peptides is best described by model 3, which invokes an effect on both bZIP dimerization and DNA binding.

The similarity between the effect of pX on ATF-2- and GCN4-derived peptides is notable in view of the lack of sequence homology between these two proteins within the bZIP element. A<sub>65</sub> and G<sub>56</sub> share only 2 of the 20 basic segment residues that do not directly contact DNA, and share only 18 of the 58 amino acids within the entire bZIP element. Despite this lack of identity, pX interacts with both peptides and has similar effects on the stabilities of the DNA complexes that they form. This correspondence suggests that pX must be capable of recognizing a broad range of amino acid sequences, or it must recognize a structural feature shared between these two peptide·CRE complexes. Recent experiments document the ability of pX to interact with different bZIP proteins lacking extensive amino acid identity (21).

**pX Recognizes bZIP·DNA Structure, Not Peptide Sequence.** To explore the role of DNA sequence and structure in pX recognition of bZIP proteins, we compared the effects of pX on the A<sub>65</sub> and G<sub>56</sub> complexes of two related but structurally distinct DNA sequences. The CRE (ATGACGTCAT) and AP-1 (ATGACTCAT) sequences are both consensus bZIP target sites. Although the sequences of these sites differ by only a single central base pair, their structures differ significantly. The available data indicate that the AP-1 target site (ATGACTCAT) exists in a structure that is very close to straight, B-form DNA (31, 46) whereas the CRE target site bends intrinsically toward the major groove (46). Both sequences bend toward the minor groove upon binding A<sub>65</sub> (D. N. Paoletta, personal communication) whereas there is no change in conformation upon binding to G<sub>56</sub> (46). Thus, to a first approximation, the CRE and AP-1 complexes of A<sub>65</sub> and GCN4 differ only in the way they present the bZIP basic segments in the major groove. If pX recognizes bZIP

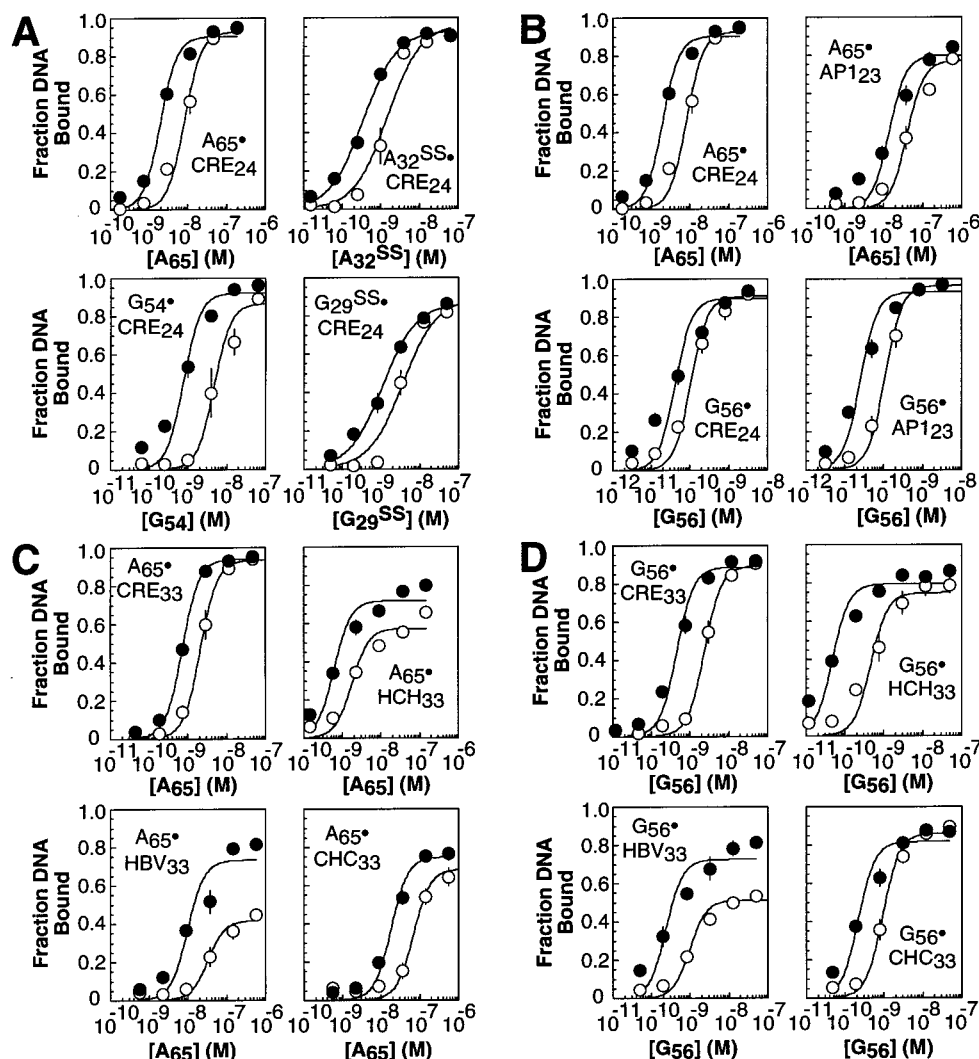


FIGURE 3: Quantitative electrophoretic mobility shift analysis of bZIP-DNA stability in the presence (filled circles) and absence (open circles) of pX. (A) Effect of pX on the CRE<sub>24</sub> affinities of A<sub>65</sub>, G<sub>56</sub>, A<sub>32</sub><sup>SS</sup>, and G<sub>29</sub><sup>SS</sup> at 4 °C. (B) Effect of pX on the CRE<sub>24</sub> and AP1<sub>23</sub> affinities of A<sub>65</sub> and G<sub>56</sub> at 4 °C. (C) Effect of pX on the affinities of A<sub>65</sub> for CRE<sub>33</sub>, HCH<sub>33</sub>, HBV<sub>33</sub>, or CHC<sub>33</sub> at 25 °C. (D) Effect of pX on the affinities of G<sub>56</sub> for CRE<sub>33</sub>, HCH<sub>33</sub>, HBV<sub>33</sub>, or CHC<sub>33</sub> at 25 °C.

Table 1: Thermodynamic Data Obtained from Electrophoretic Mobility Shift Assays<sup>a</sup>

peptide	DNA	temp (°C)	$K_d(-pX)$	$\Delta G_{obs}(-pX)$ (kcal·mol <sup>-1</sup> )	$K_d(+pX)$	$\Delta G_{obs}(+pX)$ (kcal·mol <sup>-1</sup> )	$\Delta\Delta G_{obs}$ (kcal·mol <sup>-1</sup> )
A <sub>65</sub>	CRE <sub>24</sub>	4	$(8.7 \pm 2.1) \times 10^{-17} \text{ M}^2$	-20.4	$(3.8 \pm 0.2) \times 10^{-18} \text{ M}^2$	-22.1	-1.7 ± 0.2
A <sub>32</sub> <sup>SS</sup>	CRE <sub>24</sub>	4	$(1.6 \pm 0.4) \times 10^{-9} \text{ M}$	-11.2	$(3.5 \pm 0.3) \times 10^{-10} \text{ M}$	-12.0	-0.8 ± 0.1
G <sub>54</sub>	CRE <sub>24</sub>	4	$(7.4 \pm 4.9) \times 10^{-19} \text{ M}^2$	-23.5	$(6.5 \pm 2.1) \times 10^{-21} \text{ M}^2$	-25.7	-2.2 ± 0.3
G <sub>29</sub> <sup>SS</sup>	CRE <sub>24</sub>	4	$(3.8 \pm 0.4) \times 10^{-9} \text{ M}$	-10.7	$(1.2 \pm 0.2) \times 10^{-9} \text{ M}$	-11.4	-0.7 ± 0.1
A <sub>65</sub>	CRE <sub>24</sub>	4	$(8.7 \pm 2.1) \times 10^{-17} \text{ M}^2$	-20.4	$(3.8 \pm 0.2) \times 10^{-18} \text{ M}^2$	-22.1	-1.7 ± 0.2
A <sub>65</sub>	AP1 <sub>23</sub>	4	$(2.1 \pm 0.7) \times 10^{-15} \text{ M}^2$	-18.7	$(3.0 \pm 1.2) \times 10^{-16} \text{ M}^2$	-19.8	-1.1 ± 0.1
G <sub>56</sub>	CRE <sub>24</sub>	4	$(1.2 \pm 0.3) \times 10^{-20} \text{ M}^2$	-25.3	$(1.8 \pm 0.5) \times 10^{-21} \text{ M}^2$	-26.5	-1.2 ± 0.1
G <sub>56</sub>	AP1 <sub>23</sub>	4	$(1.5 \pm 0.4) \times 10^{-20} \text{ M}^2$	-25.3	$(8.1 \pm 2.0) \times 10^{-22} \text{ M}^2$	-26.8	-1.6 ± 0.1
A <sub>65</sub>	CRE <sub>33</sub>	25	$(5.4 \pm 2.0) \times 10^{-18} \text{ M}^2$	-23.7	$(5.1 \pm 0.5) \times 10^{-19} \text{ M}^2$	-25.0	-1.3 ± 0.3
A <sub>65</sub>	HBV <sub>33</sub>	25	$(1.4 \pm 0.4) \times 10^{-15} \text{ M}^2$	-20.4	$(9.3 \pm 1.3) \times 10^{-17} \text{ M}^2$	-21.9	-1.5 ± 0.3
A <sub>65</sub>	HCH <sub>33</sub>	25	$(3.3 \pm 0.5) \times 10^{-18} \text{ M}^2$	-23.9	$(3.9 \pm 0.6) \times 10^{-19} \text{ M}^2$	-25.1	-1.3 ± 0.1
A <sub>65</sub>	CHC <sub>33</sub>	25	$(4.7 \pm 0.7) \times 10^{-15} \text{ M}^2$	-19.6	$(3.5 \pm 0.7) \times 10^{-16} \text{ M}^2$	-21.1	-1.6 ± 0.2
G <sub>56</sub>	CRE <sub>33</sub>	25	$(6.0 \pm 1.1) \times 10^{-18} \text{ M}^2$	-23.5	$(2.3 \pm 0.6) \times 10^{-19} \text{ M}^2$	-25.5	-2.0 ± 0.1
G <sub>56</sub>	HBV <sub>33</sub>	25	$(9.3 \pm 1.1) \times 10^{-19} \text{ M}^2$	-24.6	$(7.5 \pm 2.5) \times 10^{-20} \text{ M}^2$	-26.2	-1.6 ± 0.2
G <sub>56</sub>	HCH <sub>33</sub>	25	$(3.0 \pm 1.8) \times 10^{-19} \text{ M}^2$	-25.6	$(2.3 \pm 0.2) \times 10^{-21} \text{ M}^2$	-28.2	-2.6 ± 0.3
G <sub>56</sub>	CHC <sub>33</sub>	25	$(1.1 \pm 0.3) \times 10^{-18} \text{ M}^2$	-24.6	$(5.4 \pm 0.7) \times 10^{-20} \text{ M}^2$	-26.3	-1.7 ± 0.2

<sup>a</sup> Shown are the equilibrium dissociation constants ( $K_d$ ), free energies of binding in the absence [ $\Delta G_{obs}(-pX)$ ] and presence of pX [ $\Delta G_{obs}(+pX)$ ], and the increases in stability provided by pX ( $\Delta\Delta G_{obs}$ ). Values are calculated as described (43).

proteins on the basis of amino acid sequence alone, then the effect of pX on the CRE and AP-1 complexes of A<sub>65</sub> or G<sub>56</sub> should be identical. However, if pX recognizes bZIP

proteins on the basis of the structure of the bZIP-DNA complex, then the effects of pX on these peptide-DNA complexes should be different.

Binding isotherms illustrating the affinities of A<sub>65</sub> and G<sub>56</sub> for the CRE<sub>24</sub> and AP1<sub>23</sub> sites in the presence and absence of pX are shown in Figure 3B. The data show that pX has significantly different effects on the CRE and AP-1 affinities of A<sub>65</sub> and G<sub>56</sub>. pX supplemented the free energy of the A<sub>65</sub>•CRE<sub>24</sub> complex by  $\Delta\Delta G_{\text{pX}} = -1.7 \pm 0.2 \text{ kcal}\cdot\text{mol}^{-1}$  under conditions where it supplemented the free energy of the A<sub>65</sub>•AP1<sub>23</sub> complex by  $\Delta\Delta G_{\text{pX}} = -1.1 \pm 0.1 \text{ kcal}\cdot\text{mol}^{-1}$ . Similarly, pX supplemented the free energy of the G<sub>56</sub>•CRE<sub>24</sub> complex by  $\Delta\Delta G_{\text{pX}} = -1.2 \pm 0.1 \text{ kcal}\cdot\text{mol}^{-1}$  under conditions where it supplemented the binding energy of the G<sub>56</sub>•AP1<sub>23</sub> complex by  $\Delta\Delta G_{\text{pX}} = -1.6 \pm 0.2 \text{ kcal}\cdot\text{mol}^{-1}$ . Thus, pX increased the stability of the A<sub>65</sub>•CRE<sub>24</sub> complex more than the A<sub>65</sub>•AP1<sub>23</sub> complex but increased the stability of the G<sub>56</sub>•AP1<sub>23</sub> complex more than the G<sub>56</sub>•CRE<sub>24</sub> complex. The observation that pX had different effects on the stabilities of complexes containing the same peptide but a different DNA sequence (and structure) supports a model in which pX recognizes a distinct bZIP•DNA structure, and not simply bZIP peptide sequence. The differential effects of pX on the CRE and AP-1 complexes of A<sub>65</sub> result in a 3-fold increase in the selectivity of this peptide for its cognate CRE target site. This change in specificity may be related to the ability of pX to deregulate cellular transcription of CRE-dependent genes.

**Contribution of Extended DNA Structure to pX Enhancement.** *In vivo*, pX enhances transcription from a variety of DNA target sites, including a 21 bp HBV enhancer located upstream of the *X* gene (47, 48). Contained within this enhancer is an imperfect 10 bp CRE site core (CTGACG-CAAC) surrounded by distinctive flanking sequences of unknown function. These flanking sequences resemble those found in other viral long terminal repeats, including the Tax response elements from HTLV-I (12, 49). The Tax response elements and the hepatitis B virus enhancer both contain 4–5 cytosine residues located immediately 3' to the CRE-like core. Previous results have demonstrated that the flanking sequences in the HTLV-I enhancer alter the structure of the central CRE core in the absence of a bound bZIP peptide and the recognition of this sequence by bZIP peptides and HTLV-I Tax (49–51).

To investigate the role of the flanking DNA in modulating pX•bZIP interactions, we measured the effect of pX on the bZIP affinities of four different DNA target sites: a consensus CRE site (CRE<sub>33</sub>), a HBV enhancer site (HBV<sub>33</sub>), and two chimeric sites containing either a 10 bp consensus CRE core and the flanking sequences found in the HBV enhancer (HCH<sub>33</sub>) or the 10 bp imperfect CRE core found in the HBV enhancer and the CRE flanking sequences (CHC<sub>33</sub>). Binding isotherms illustrating the affinities of A<sub>65</sub> for each of these DNA sequences in the presence and absence of pX are shown in Figure 3C.

First consider the role of flanking DNA in bZIP recognition in the absence of pX. In the absence of pX, A<sub>65</sub> bound CRE<sub>33</sub> with considerably higher affinity ( $\Delta G_{\text{CRE}} = -23.7 \text{ kcal}\cdot\text{mol}^{-1}$ ) than it bound HBV<sub>33</sub> ( $\Delta G_{\text{HBV}} = -20.4 \text{ kcal}\cdot\text{mol}^{-1}$ ). This difference in affinity was due entirely to recognition of the central CRE-like core; the stability of the A<sub>65</sub>•CRE<sub>33</sub> complex ( $\Delta G_{\text{CRE}} = -23.7 \text{ kcal}\cdot\text{mol}^{-1}$ ) was comparable to that of the A<sub>65</sub>•HCH<sub>33</sub> complex ( $\Delta G_{\text{HCH}} = -23.9 \text{ kcal}\cdot\text{mol}^{-1}$ ), and the stability of the A<sub>65</sub>•HBV<sub>33</sub> complex ( $\Delta G_{\text{HBV}} = -20.4 \text{ kcal}\cdot\text{mol}^{-1}$ ) was comparable to that of the A<sub>65</sub>•CHC<sub>33</sub> ( $\Delta G_{\text{CHC}} = -19.6 \text{ kcal}\cdot\text{mol}^{-1}$ ) complex.

These data suggest that A<sub>65</sub> is insensitive to the identity of the flanking DNA in the absence of pX. These sequences neither modulate DNA structure in a manner that is detectable by A<sub>65</sub> nor present additional contacts that improve binding. Similar results are observed in the presence of pX. The pX-induced increase in stability was nearly identical for all four A<sub>65</sub>•DNA complexes, and as a result, the relative stabilities of the four A<sub>65</sub>•DNA complexes did not change. We conclude that recognition of the A<sub>65</sub>•DNA complex by pX is mediated by recognition of the core peptide•DNA complex and is not affected by flanking DNA. This conclusion is consistent with DNase I footprinting experiments performed with pX and full-length ATF-2 (17) as well as methylation interference experiments performed with pX and CREB (16).

Although pX recognition of A<sub>65</sub>•DNA complexes was insensitive to flanking DNA sequence, pX recognition of G<sub>56</sub>•DNA complexes was not. Binding isotherms illustrating the affinity of G<sub>56</sub> for the CRE<sub>33</sub>, HBV<sub>33</sub>, HCH<sub>33</sub>, and CHC<sub>33</sub> target sites in the absence and presence of pX are shown in Figure 3D. In the absence of pX, G<sub>56</sub> bound HBV<sub>33</sub> with slightly higher affinity ( $\Delta G_{\text{HBV}} = -24.6 \text{ kcal}\cdot\text{mol}^{-1}$ ) than it bound CRE<sub>33</sub> ( $\Delta G_{\text{CRE}} = -23.5 \text{ kcal}\cdot\text{mol}^{-1}$ ). This difference in affinity was due to recognition of the entire HBV sequence: Although the stability of the G<sub>56</sub>•HBV<sub>33</sub> complex ( $\Delta G_{\text{HBV}} = -24.6 \text{ kcal}\cdot\text{mol}^{-1}$ ) was identical to that of the G<sub>56</sub>•CHC<sub>33</sub> complex ( $\Delta G_{\text{HCH}} = -24.6 \text{ kcal}\cdot\text{mol}^{-1}$ ), both complexes were significantly less stable than the G<sub>56</sub>•HCH<sub>33</sub> complex ( $\Delta G_{\text{HCH}} = -25.6 \text{ kcal}\cdot\text{mol}^{-1}$ ). The relative affinities of the four G<sub>56</sub>•DNA complexes were unchanged in the presence of pX. The G<sub>56</sub>•HBV<sub>33</sub> and G<sub>56</sub>•CHC<sub>33</sub> complexes exhibited nearly identical stabilities ( $\Delta G_{\text{HBV}} = -26.2 \text{ kcal}\cdot\text{mol}^{-1}$ ;  $\Delta G_{\text{HCH}} = -26.3 \text{ kcal}\cdot\text{mol}^{-1}$ ) whereas the G<sub>56</sub>•HCH<sub>33</sub> complex was considerably more stable ( $\Delta G_{\text{HCH}} = -28.2 \text{ kcal}\cdot\text{mol}^{-1}$ ). The data suggest that pX increases the affinity of a bZIP peptide for the DNA sequence bound in the absence of pX but does not induce additional DNA contacts. These results are consistent with model 3 in which pX recognizes the structure of the DNA-bound bZIP protein.

## DISCUSSION

In this paper, we explore the molecular mechanism by which HBV pX increases the DNA affinities of certain bZIP peptides at equilibrium. We proposed that this increase in affinity could arise in three different ways: from an increase in stability of the bZIP•bZIP interaction (model 1), an increase in stability of the bZIP•DNA interaction (model 2), or both (case 3) (43). These three possibilities are illustrated as reaction coordinate diagrams in Figure 1 for a binding pathway in which dimerization precedes DNA binding (52). In each case, if pX increases the equilibrium stability of a bZIP•DNA complex, then it must participate in a ternary pX•bZIP•DNA complex that is more stable than the bZIP•DNA complex alone. This statement is true, and applies equally to other related proteins, even if the complex is difficult to observe. The only way by which pX could stabilize a protein•DNA complex without formation of a ternary complex is by destabilizing the protein before it binds DNA. Although this mechanism represents a formal possibility, it is unlikely because only a scant amount of the destabilized species would exist in solution and we do not consider the possibility here. The observation that pX increases the DNA affinities of the disulfide dimer peptides, A<sub>32</sub><sup>SS</sup> and G<sub>29</sub><sup>SS</sup>, by values lower than those observed with

the corresponding bZIP element peptides supports a model in which both dimerization and DNA binding are affected by pX. It also confirms that the basic-spacer segment is the predominant site of interaction with pX, a conclusion which is consistent with earlier results (16).

How might pX interact with the bZIP basic-spacer segment to increase both DNA binding and dimerization? The basic segments of bZIP proteins are unstructured in the absence of DNA (53–56), and become fully helical only upon binding to a specific DNA target sequence (56, 57). Therefore, the observed increase in DNA binding could result from an interaction between pX and the outside surface of the bZIP•DNA complex that stabilizes this fully helical conformation. It has been estimated to cost roughly 1.8 kcal•mol<sup>-1</sup> ( $-T\Delta S$ ) to convert one residue from an unordered state into a helical state upon DNA binding (58). Thus, the 2–3 kcal•mol<sup>-1</sup> enhancement in bZIP•DNA stability with pX would offset a fraction of the total entropy change required for folding of the bZIP basic segment. Alternatively, pX could orient the peptide helices in the DNA major groove (40), or alter the conformation of the peptide helix to accommodate additional DNA contacts. The observed increase in bZIP dimerization with pX could arise from a helical templating effect in which induced helicity within the basic or spacer segments is propagated through the zipper segment. Alternatively, some fraction of the total enhancement may result from stabilization of helical structure caused by a direct interaction between pX and the zipper segment.

How might pX recognize the structure of the bZIP•DNA complex, and not the sequence of the bZIP protein? Although bZIP proteins that interact with pX share few residues that do not participate in base-specific DNA contacts, they do share an extensive array of lysine and arginine residues that contact the phosphodiester backbone. These contacts exist in all bZIP•DNA complexes, but the precise number and arrangement of these contacts likely differ. One possibility is that pX recognizes the pattern of basic side chain•phosphate contacts that positions the basic segment helix in the DNA major groove. Even if other factors contribute, this model would provide an explanation for the ability of pX to interact with bZIP proteins that lack identity at the level of primary sequence. In spite of its evolutionary advantage to the virus, this mechanism of recognition provides a testable strategy for inhibition of pX function.

Our results regarding the effects of pX on bZIP peptides mirror results obtained with another viral transcriptional activator, the Tax protein of HTLV-I. Like pX, Tax activates transcription of CRE-dependent genes through a direct Tax•bZIP interaction. Like Tax, pX interacts predominantly with the bZIP basic-spacer segment to enhance DNA binding (34, 43, 59) and discriminates between peptide•DNA complexes based upon the identity of the DNA target site (49). In spite of the similarities in their functions *in vitro* and *in vivo*, Tax and pX exhibit no homology at the level of primary sequence. Not only are these proteins not obviously homologous to one another, they are also not homologous to any protein in the Genbank nonredundant database. The observation that these two viral accessory proteins share a common mode of interaction in the absence of obvious sequence homology suggests that the homology is present but obscure, or that these proteins have converged through

evolution to two different structures capable of performing a similar function *in vivo*.

## ACKNOWLEDGMENT

We thank A. Baranger, S. Metallo, N. Zondlo, and J. Janin for comments and discussion. High-resolution mass spectra were obtained in the Mass Spectrometry Laboratory, School of Chemical Sciences, University of Illinois, using a ToFSpec mass spectrometer which was purchased in part with a grant from the Division of Research Resources, National Institutes of Health (RR 07141).

## REFERENCES

- Ganem, D., and Varmus, H. E. (1987) *Annu. Rev. Biochem.* 56, 651–693.
- Böttcher, B., Wynne, S. A., and Crowther, R. A. (1997) *Nature* 386, 88–91.
- Conway, J. F., Cheng, N., Zlotnick, A., Wingfield, P. T., Stahl, S. J., and Steven, A. C. (1997) *Nature* 386, 91–94.
- Hirsch, R. C., Lavine, J. E., Chang, L. J., Varmus, H. E., and Ganem, D. (1990) *Nature* 344, 552–555.
- Tiollais, P., Pourcel, C., and Dejean, A. (1985) *Nature* 317, 489–495.
- Luber, B., Arnold, N., Stürzl, M., Höhne, M., Schirmacher, P., Lauer, U., Weinberg, J., Hofschneider, P. H., and Kekulé, A. S. (1996) *Oncogene* 12, 1597–1608.
- Robinson, W. S. (1994) *Annu. Rev. Med.* 45, 297–323.
- Doria, M., Klein, N., Lucito, R., and Schneider, R. J. (1995) *EMBO J.* 14, 4747–4757.
- Benn, J., and Schneider, R. J. (1994) *Proc. Natl. Acad. Sci. U.S.A.* 91, 10350–10354.
- Avantaggiati, M. L., Natoli, G., Balsano, C., Chirillo, P., Artini, M., De Marzio, E., Collepardo, D., and Levrero, M. (1993) *Oncogene* 8, 1567–1574.
- Mahé, Y., Mukaidas, N., Kuno, K., Akiyama, M., Ikeda, N., Matsushima, K., and Murakami, S. (1991) *J. Biol. Chem.* 266, 13759–13763.
- Faktor, O., and Shaul, Y. (1990) *Oncogene* 5, 867–872.
- Seto, E., Mitchell, P. J., and Yen, T. S. B. (1990) *Nature* 344, 72–74.
- Spandau, D. F., and Lee, C.-H. (1988) *J. Virol.* 62, 427–434.
- Ben-Levy, R., Faktor, O., Berger, I., and Shaul, Y. (1989) *Mol. Cell. Biol.* 9, 1804–1809.
- Williams, J. S., and Andrisani, O. M. (1995) *Proc. Natl. Acad. Sci. U.S.A.* 92, 3819–3923.
- Maguire, H. F., Hoeffler, J. P., and Siddiqui, A. (1991) *Science* 252, 842–844.
- Wang, X. W., Forrester, K., Yeh, H., Feitelson, M. A., Gu, J.-R., and Harris, C. C. (1994) *Proc. Natl. Acad. Sci. U.S.A.* 91, 2230–2234.
- Qadri, I., Maguire, H. F., and Siddiqui, A. (1995) *Proc. Natl. Acad. Sci. U.S.A.* 92, 1003–1007.
- Cheong, J., Yi, M., Lin, Y., and Murakami, S. (1995) *EMBO J.* 14, 143–150.
- Barnabas, S., Hai, T., and Andrisani, O. M. (1997) *J. Biol. Chem.* 272, 20684–20690.
- Qadri, I., Ferrari, M. E., and Siddiqui, A. (1996) *J. Biol. Chem.* 271, 15443–15450.
- Unger, T., and Shaul, Y. (1990) *EMBO J.* 9, 1889–1895.
- McKnight, S. L. (1991) *Sci. Am.* 264, 54–64.
- Hurst, H. C. (1994) *Protein Profile* 1, 123–168.
- Hurst, H. C. (1995) *Protein Profile* 2, 101–168.
- Hai, T., Liu, F., Coukos, J., and Green, M. R. (1989) *Genes Dev.* 3, 2083–2090.
- Habener, J. F. (1990) *Mol. Endocrinol.* 4, 1087–1094.
- Lee, K. A. W., and Masson, N. (1993) *Biochim. Biophys. Acta* 1174, 221–233.
- Harrison, S. C. (1991) *Nature* 353, 715–719.
- Ellenberger, T. E., Brandl, C. J., Struhl, K., and Harrison, S. C. (1992) *Cell* 71, 1223–1237.
- Glover, J. N. M., and Harrison, S. C. (1995) *Nature* 373, 257–261.

33. Keller, W., König, P., and Richmond, T. J. (1995) *J. Mol. Biol.* 254, 657–667.
34. Wagner, S., and Green, M. R. (1993) *Science* 262, 395–399.
35. Natoli, G. A., Avantiaggiati, M. L., Chirillo, P., Costanzo, A., Artini, M., Balsano, C., and Levrero, M. (1994) *Mol. Cell. Biol.* 14, 989–998.
36. Balsano, C., Billet, O., Bennoun, M., Cavard, C., Zider, A., Grimber, G., Natoli, G., Briand, P., and Levrero, M. (1994) *J. Hepatol.* 21, 103–109.
37. Wu, J. Y., Zhou, Z.-Y., Judd, A., Cartwright, C. A., and Robinson, W. S. (1990) *Cell* 63, 687–695.
38. Metallo, S. J., and Schepartz, A. (1994) *Chem. Biol.* 1, 143–151.
39. Cuenoud, B., and Schepartz, A. (1993) *Proc. Natl. Acad. Sci. U.S.A.* 90, 1154–1159.
40. Cuenoud, B., and Schepartz, A. (1993) *Science* 259, 510–513.
41. Maniatis, T., Fritsch, E. F., and Sambrook, J. (1987) *Molecular Cloning: A Laboratory Manual*, 2nd ed., Cold Spring Harbor Press, Cold Spring Harbor, NY.
42. Stewart, J. M., and Young, J. D. (1984) *Solid Phase Peptide Synthesis*, Raven Press, New York.
43. Baranger, A. M., Palmer, C. R., Hamm, M. K., Giebler, H. A., Brauweiler, A., Nyborg, J. K., and Schepartz, A. (1995) *Nature* 376, 606–608.
44. Du, W., and Maniatis, T. (1992) *Proc. Natl. Acad. Sci. U.S.A.* 89, 2150–2154.
45. Hinnebusch, A. G., and Fink, G. R. (1983) *Proc. Natl. Acad. Sci. U.S.A.* 80, 5374–5378.
46. Paolella, D. N., Palmer, C. R., and Schepartz, A. (1994) *Science* 264, 1130–1133.
47. Patel, N. U., Jameel, S., Isom, H., and Siddiqui, A. (1989) *J. Virol.* 63, 5293–5301.
48. Guo, W., Bell, K. D., and Ou, J.-H. (1991) *J. Virol.* 65, 6686–6692.
49. Cox, J. M., Sloan, L. S., and Schepartz, A. (1995) *Chem. Biol.* 2, 819–826.
50. Paca-Uccaralertkun, S., Zhao, L. J., Adya, N., Cross, J. V., Cullen, B. R., Boros, I. M., and Giam, C. Z. (1994) *Mol. Cell. Biol.* 14, 456–462.
51. Yin, M. J., and Gaynor, R. B. (1996) *J. Mol. Biol.* 264, 20–31.
52. Metallo, S. J., and Schepartz, A. (1997) *Nat. Struct. Biol.* 4, 115–117.
53. Weiss, M. (1990) *Biochemistry* 29, 8020–8024.
54. Weiss, M. A., Ellenberger, T., Wobbe, C. R., Lee, J. P., Harrison, S. C., and Struhl, K. (1990) *Nature* 347, 575–578.
55. O'Neil, K. T., Hoess, R. H., and DeGrado, W. F. (1990) *Science* 249, 774–778.
56. O'Neil, K. T., Shuman, J. D., Ampe, C., and DeGrado, W. F. (1991) *Biochemistry* 30, 9030–9034.
57. Johnson, N. P., Lindstrom, J., Baase, W. A., and von Hippel, P. H. (1994) *Proc. Natl. Acad. Sci. U.S.A.* 91, 4840–4844.
58. Spolar, R., and Record, M. T., Jr. (1994) *Science* 263, 777–784.
59. Perini, G., Wagner, S., and Green, M. R. (1995) *Nature* 376, 602–605.
60. König, P., and Richmond, T. (1993) *J. Mol. Biol.* 233, 139–154.
61. O'Shea, E. K., Klemm, J. D., Kim, P. S., and Alber, T. (1991) *Science* 254, 539–544.
62. Talanian, R. V., McKnight, C. J., Rutkowski, R., and Kim, P. S. (1992) *Biochemistry* 31, 6871–6875.
63. Talanian, R. V., McKnight, C. J., and Kim, P. S. (1990) *Science* 249, 769–771.
64. Pu, W. T., and Struhl, K. (1991) *Proc. Natl. Acad. Sci. U.S.A.* 88, 6901–6905.
65. Vinson, C. R., Sigler, P. B., and McKnight, S. L. (1989) *Science* 246, 911–916.
66. Johnson, P. F. (1993) *Mol. Cell. Biol.* 13, 6919–6930.
67. Kim, J., and Struhl, K. (1995) *Nucleic Acids Res.* 23, 2531–2537.

BI972076M